

Ultraviolet radiation produced in low-energy Ar + Ar and Kr + Kr collisions

H. L. Rothwell, Jr.,* R. C. Amme, and B. Van Zyl

Department of Physics, University of Denver, Denver, Colorado 80208

(Received 18 September 1978)

Absolute cross sections for the emission of ultraviolet resonance line radiations from Ar and Kr atoms resulting from Ar + Ar and Kr + Kr collisions are reported. The energy range covered extends from near the reaction thresholds to 150 eV in the center-of-mass system. The emission cross sections are found to have energy dependencies very similar to those exhibited by the total ionization cross sections for the same reactants. The techniques used to make the measurements are described and the results are discussed in terms of a current theoretical model of the interactions.

I. INTRODUCTION

In a recent preliminary disclosure,¹ we published the results of measurements of the resonance-line emission cross sections for low-energy Ar + Ar collisions between ground-state atoms. These results have now been substantiated and extended to include data from Kr + Kr interactions. The findings are here described in detail together with a review of the techniques employed to accomplish the measurements.

The lowest excited states of the Ar and Kr atoms are formed from the $3p^5 4s$ and $4p^5 5s$ configurations, respectively. These configurations each form a quartet of levels, two of which are metastable and two of which decay optically at the resonance line wavelengths of 104.8 and 106.7 nm for Ar and 116.5 and 123.6 nm for Kr. These were the radiations observed in the present experiments. Their emission cross sections were measured from near the excitation thresholds to 150 eV in the center of mass system.

The production of guaranteed ground-state atomic beams of Ar and Kr atoms in this low-energy region requires considerable care. In addition to the usual requirements of a neutral beam of known intensity and sufficient collimation to perform the measurements, the beam must not be allowed to

contain excited metastable atoms. It will be shown that the presence of even a very small fraction of such atoms in the atomic beam can have a profound effect on the measurements reported here. The techniques used to generate the guaranteed ground-state Ar and Kr atomic beams are discussed in Sec. III, following a description of the apparatus found in Sec. II.

The ultraviolet (uv) radiation detectors and their absolute calibrations are discussed in Sec. IV. The results of the emission cross section measurements are presented in Sec. V together with a limited amount of data for Ar + Kr and Kr + Ar collisions. A discussion of all results is found in Sec. VI where the present data are compared with other processes involving the same reactants and are considered in the light of current theoretical understanding of such reactions.

II. EXPERIMENTAL APPARATUS

The basic ion source, electrostatic lens assembly, and charge exchange neutralization cell have been described earlier² and will be only briefly reviewed here. The ion lens assembly has been modified to improve focusing at ion energies below 50 eV. The entire neutral atom accelerator is schematically represented in Fig. 1.

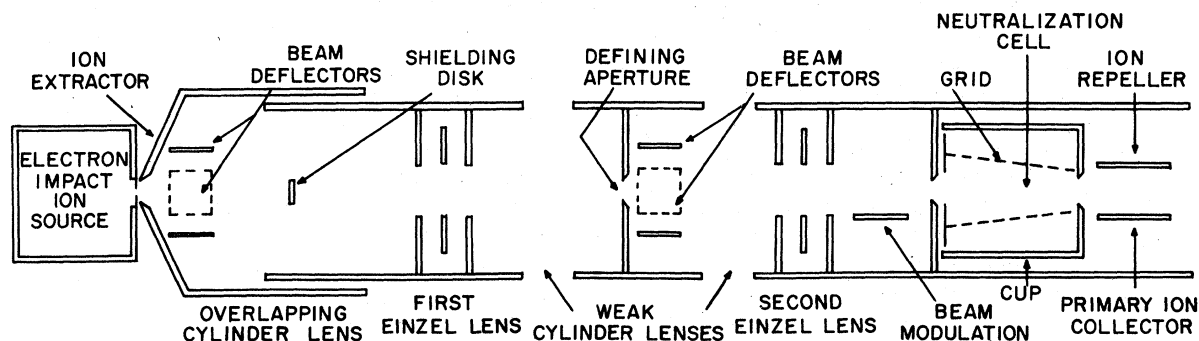


FIG. 1. Neutral atom accelerator.

Ions are produced by electron bombardment in a low pressure (typically 10^{-2} Torr) ion source. The electron accelerating voltage is continuously variable, with an electron energy distribution width of about 1.5-eV full width at half-maximum (FWHM). The electron energy is maintained low enough to avoid production of excited electronic states of the primary Ar^+ and Kr^+ ions.³

Ions are extracted from the source through a 0.3-mm diam aperture in thin fold foil. Initial focusing is accomplished by an overlapping cylindrical lens followed by a three element Einzel lens to direct the ions through a 2.0-mm diam defining aperture. This aperture partially shields the neutralization cell from stray neutrals (some at high energy) produced in the ion source exit and extraction regions. Additional shielding is provided by a small (3-mm diam) disk positioned on the beam axis at the principal plane of the overlapping cylindrical lens. Ions emerging from the defining aperture are then focused into the neutralization cell with the aid of a weak cylinder lens and a second Einzel lens.

The neutralization cell consists of a cylindrical metallic cup with an electrically isolated wire grid which is cylindrically coaxial to the cup and ion beam axis. The cup is maintained at about 2×10^{-4} Torr pressure of the charge transfer gas. Slow target ions produced in a resonant or near-resonant charge exchange with the incident beam ions are collected on the grid by applying a small retarding potential to the cup. For single electron transfer, the number of slow ions collected is directly proportional to the number of fast neutrals formed. Typically 5%-15% of the fast ions are neutralized, and the remaining ions are swept clear of the neutral beam at the ion collector station after exiting the neutralization cell.

The collimated neutrals (or primary ions, for some experiments) enter the target scattering region shown schematically in Fig. 2. In this low pressure cell (typically held between 1 and 3×10^{-4} Torr as measured to within $\pm 10\%$ by a capacitance diaphragm manometer), ultraviolet light from atomic collisions can be studied with the aid of two detectors, both of which view the atomic beam normal to its direction of motion.

The "total uv detector" consists of two defining apertures (one square and one circular), a thin LiF window, and a commercial Channeltron multiplier (CEM) operating in a pulse-counting mode. The LiF window (to keep charged particles from the CEM surface) and the CEM combine to give this detector an effective bandpass from 104 to 125 nm. The second detector is a near normal incidence grating monochromator. The grating is a holographic spherical type with 0.3-m radius.

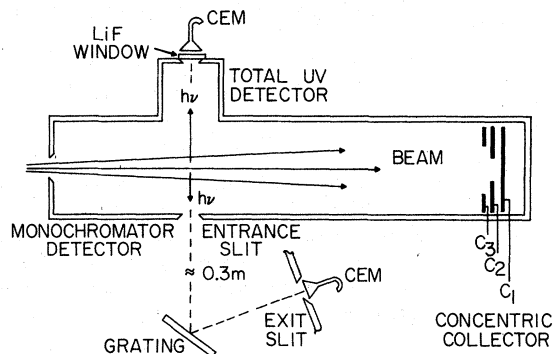


FIG. 2. Target scattering cell.

With entrance and exit slits of 0.5×10 mm this instrument has a resolution of about 1 nm. Another CEM is positioned behind the exit slit to monitor the radiation at the dispersed wavelength.

To enhance the signal to background separation, the primary ion flux (and hence the neutral flux as well) is modulated by application of a 50% duty cycle, 40-Hz square wave deflection potential in front of the neutralization cell. Two counters sharing an input from the same CEM are gated in/out of phase with the applied potential such that one counter detects the sum of signal plus background counts and the other background counts ($\sim 0.05/\text{sec}$) only. Because of the small signal levels at the low energies, hours of accumulation time were needed to reach 5% counting statistics.

At the rear of the target cell is situated a segmented collector of concentric symmetry to allow an evaluation of the beam profile and extent. For example, any fast particle leaving the neutralization cell and arriving at the center segment C_1 must have passed through the viewing fields of both detectors. On the other hand, only about 43% of the fast particles reaching segment C_2 and 22% of those reaching C_3 will pass through the field of the monochromator detector,⁴ even though they all are viewed by the total uv detector. Finally, at the lowest energies (28 eV was the lowest laboratory energy used in these studies), only about two thirds of the particles leaving the charge transfer neutralization cell can be made to enter the target cell via its restrictive (differential pumping) front aperture.

For experiments with ion projectiles, this situation constitutes no problem as ion current measurements at the various electrodes can be used to determine directly the relative amounts of the total ion flux being viewed by the two detectors. Down to about 70 eV, it is also possible to scan the neutral beam profile with a CEM. At lower energies, however, the secondary electron emission coefficient from the CEM surface was too

small to allow such studies.

At 70 eV, the neutral beam profile is nicely peaked on the beam axis with an extent comparable to or smaller than the corresponding primary ion profile. This is not surprising since the elastic scattering of these two species as they move from the neutralization cell to the target cell is probably comparable, and the neutrals are not subject to space-charge or stray electric or magnetic field defocussing of their trajectories. In addition, the neutralization reaction itself (see discussion in Sec. III) is not expected to result in substantial angular spread for the reactions employed here.

In view of these considerations, it is here assumed that, even at the lower energies, the spatial profile and extent of the neutral beam are no worse than those of the primary ions. Nevertheless, increased uncertainty from this assumption must be included for the lower energies.

III. GROUND-STATE NEUTRAL BEAM FORMATION

In many experiments, the symmetric resonant charge transfer process, (i.e., $\text{Ar}^+ + \text{Ar}$ or $\text{Kr}^+ + \text{Kr}$) is used to neutralize parent ions because of the large ($\sim 10^{-15} \text{ cm}^2$) cross section for the process at low energies. Since the reaction is resonant, the resulting neutrals are expected to have nearly the same energy and momentum distribution as the primary ions.

For such equal mass species, however, the energy required in the laboratory system for exciting the product neutral atom in the charge exchange is only twice the excitation energy for production of the excited state involved. Thus above 23 eV for Ar^+ and 20 eV for Kr^+ , the symmetric neutralization process can leave some of the product neutrals excited. As mentioned in Sec. I, both Ar and Kr have low-lying metastable states, which can contaminate the desired ground-state neutral beam.

The production of metastable Ar atoms in low-energy $\text{Ar}^+ + \text{Ar}$ charge exchange reactions has been reported,⁵ with the ratio of metastable state to ground state formation being estimated to be about $1/10^4$. A similar situation results for the $\text{Kr}^+ + \text{Kr}$ neutralization. It will be shown in Sec. V that the use of such neutral beams, even though their metastable atom component is very small, can lead to significant error in the measurement of near-threshold emission cross sections.

To avoid this problem, the primary Ar^+ ions are here neutralized in H_2 gas. This charge transfer cross section is large down to below 50 eV.⁶ In addition, the low mass of this target very much minimizes the angular divergence of the product

neutral beam. But, most importantly, the large mass difference prevents population of an excited Ar atom state (requiring 11.5 eV center-of-mass energy) until laboratory Ar^+ energies in excess of 200 eV have been surpassed.

For Kr^+ neutralization, molecular hydrogen is not a suitable charge-transfer target. We have found, however, that CO appears nearly resonant for neutralization of Kr^+ ions. The charge-transfer cross section for the $\text{Kr}^+ + \text{CO}$ system has been measured using an ion source electron energy of 27 eV, below the threshold for excited Kr^+ ion formation. The results of this study are presented in Fig. 3 where the older data for $\text{Ar}^+ + \text{H}_2$ are included for comparison.⁶ Using CO as the charge-transfer medium guarantees ground state Kr atom formation for Kr^+ ion energies below approximately 40 eV, well above the threshold region of primary interest here. The uncertainties present in these charge transfer cross section measurements are judged to be $\pm 15\%$.

Even by using these charge-transfer gas combinations, however, difficulties can be encountered if the ion source electron energy is allowed to exceed that energy at which excited metastable Ar^+ and Kr^+ ions can be formed.³ For the case of the $\text{Ar}^+ + \text{H}_2$ neutralization, we have recently shown that metastable Ar^+ ions can charge transfer in H_2 to yield metastable neutral Ar atoms.⁷ Thus both the ion source electron energy and the charge transfer gas partner must be carefully selected to guarantee the production of ground-state neutral Ar and Kr atom beams.

The uncertainties in the neutral atom beam flux are estimated to be $\pm 15\%$ down to 50-eV ion ener-

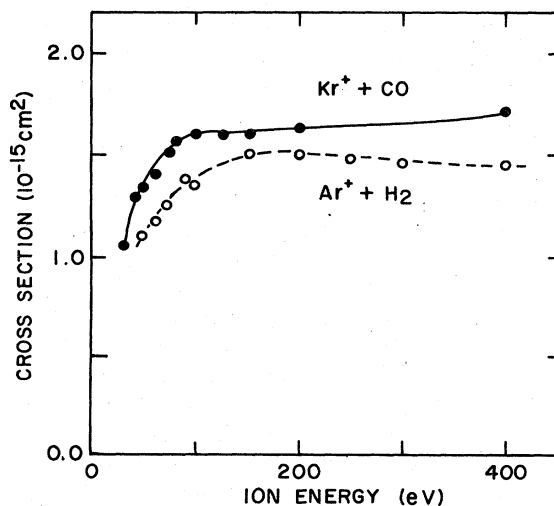


FIG. 3. Charge transfer cross section for Kr^+ ions in CO targets. The $\text{Ar}^+ + \text{H}_2$ charge transfer cross section (from Ref. 6) is shown for comparison.

gy, below which they increase inversely with ion energy to about twice this value at 28 eV.

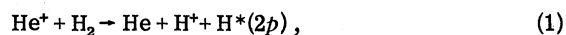
IV. ABSOLUTE DETECTOR CALIBRATIONS

The total uv detector, consisting of two limiting apertures, the LiF window,⁸ and the CEM, subtends a solid angle of approximately 2×10^{-3} sr from the neutral beam axis. This solid angle was numerically computed and averaged over the neutral beam profile, weighted by the ratios of the primary ion current measurements to the segmented collector electrodes. The uncertainty in determining an effective solid angle from this procedure is judged to be $\pm 10\%$.

The wavelength dependence of the LiF window transmission was measured directly from a comparison of the CEM signal with and without the window covering the exit slit of the monochromator. The transmission ranged from 0.30 at 104.8 nm to 0.95 at 123.6 nm, with a measurement uncertainty of about $\pm 10\%$. The quantum efficiency of the CEM was estimated to be about 0.06 and 0.02 at these same wavelengths, respectively. These data were obtained from typical results for similar devices,⁹ and are here taken to be uncertain by $\pm 20\%$.

Combination of these various uncertainties in quadrature gives a net uncertainty of about $\pm 25\%$ for the absolute detector calibration sensitivity. Except at the very low energies where the neutral beam flux is more uncertain, this value gave rise to a total uncertainty of $\pm 30\%$ for a cross section determination with the absolute beam flux and target gas density uncertainties again being added in quadrature to the detector calibration uncertainty.

To check the total uv detector efficiency determined above, the cross section for emission of Lyman-alpha radiation (121.6 nm) from the reaction



was measured for 300-eV He⁺ energy. (Prior to the measurement, the 104–125 nm bandpass region of this total uv detector was scanned with the monochromator detector to verify the absence of other significant radiation.) The cross section value obtained was 5.3×10^{-17} cm², about 15% below the published value of Dunn, Geballe, and Pretzer,¹⁰ well within the combined uncertainty of the two measurements.

A similar procedure was employed to estimate the efficiency of the monochromator detector, although substantially larger uncertainties are involved. Here, the solid angle is only about 10^{-5} sr and only crude estimates were available for the

efficiencies of the various components comprising this detector. Nevertheless, the cross section for reaction (1) was determined with the monochromator detector for He⁺ energies of 50, 100, 300, and 500 eV. The results obtained were $15\% \pm 7\%$ above those found by Dunn *et al.*

In view of the large uncertainties involved with absolute use of the monochromator detector, this agreement is fortuitous. The important result is that the observed energy dependence of the cross section closely duplicates that reported by Dunn *et al.* Since the ratios of the currents to the various concentric collectors at the rear of the target cell (see Fig. 2.) varied with beam energy (and therefore the fraction of the He⁺ ions passing within this detector's viewing field), it appears that the correction to the measured data for this effect can be properly executed.

In view of the considerable uncertainty associated with the monochromator detector efficiency determination, the absolute cross section data obtained with this detector were normalized to those obtained with the total uv detector.

V. RESULTS OF THE MEASUREMENTS

A monochromator scan of the uv emission produced in 150-eV center-of-mass Kr+Kr collisions is shown in Fig. 4. These raw data display the monochromator resolution and the absence of any other radiations within the bandpass of the total uv detector (the region between 104 and 125 nm). The 116.5- and 123.6-nm resonance lines from the Kr atom are well above the background level. (On the other hand, the next group of excited states of the Kr atom radiate in the 100- to 105-nm region, within the spectral response region of the monochromator detector. In spite of a lengthy search for signal in this region, no discernible

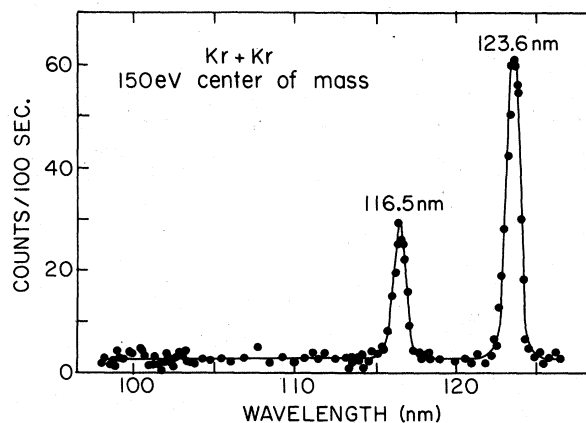


FIG. 4. Monochromator detector scan of the uv radiation from Kr + Kr collisions.

emissions above reasonable background scatter were identified.) This type of data, when combined with the CEM efficiency as a function of wavelength, allowed determination of the relative emission intensity for the two lines observed.¹¹

The measured uv emission cross sections for Ar + Ar collisions are shown in Fig. 5. The upper curve shows the absolute cross sections as determined with the total uv detector. The lower two curves are the (normalized) spectrally resolved data obtained with the monochromator detector. These results extend only down to 30-eV center-of-mass energy, below which the signal was too small to be measured with this detector. (The dashed curve is the total ionization cross section to be discussed in Sec. VI). Figure 6 shows the comparable data obtained for the case of Kr + Kr collisions.

Note that for both reactions, the relative emission intensities of the two resonance line radiations are essentially constant. Thus the intensity ratio $I(104.8)/I(106.7) = 0.71 \pm 10\%$ for Ar collisions over the entire energy range covered. The Kr data show the ratio $I(116.5)/I(123.6) = 0.22 \pm 10\%$, again being the same at all energies.

A limited amount of data were also obtained for these intensity ratios for Ar + Kr and Kr + Ar collisions, which are, of course, identical collisions in the center-of-mass system. The observed intensity ratios were $I(104.8)/I(106.7) = 0.66$ and

0.72 , and $I(116.5)/I(123.6) = 0.21$ and 0.18 , respectively. Thus the same ratios, within uncertainties, are found even for such nonsymmetric reactions. In fact, the ratio $I(104.8)/I(106.7)$ was found to be ≈ 0.6 even for $\text{Ar}^+ + \text{Ar}$ reactions, thereby persisting at about the same value for the case of ion impact.

Figure 7 show the total uv emission cross sections for Ar + Ar and Kr + Kr collisions in the threshold regions. In Figs. 7(a) and 7(c), the lower curves are the results obtained for ground-state beam atoms (i.e., for Ar^+ neutralized in H_2 and Kr^+ neutralized in CO), while the upper curves indicate the data from symmetric-resonant ion neutralization (Ar^+ in Ar and Kr^+ in Kr). Figures 7(b) and 7(d) show the same regions over an expanded range.

The energy scale in Figs. 7 has been corrected by about 0.7 eV as a result of a retarding potential analysis of the primary ions. We have assumed that the same correction must apply to the neutral beam atoms. This analysis also revealed that the primary ion energy distribution had a FWHM spread of about 0.5-eV center-of-mass energy, and a comparable spread was assumed for the neutral beam atoms. In view of these and other considerations, an energy uncertainty of ± 2 eV must be assigned to these data.

It is quite apparent that the neutral beams obtained by using the symmetric-resonant charge-

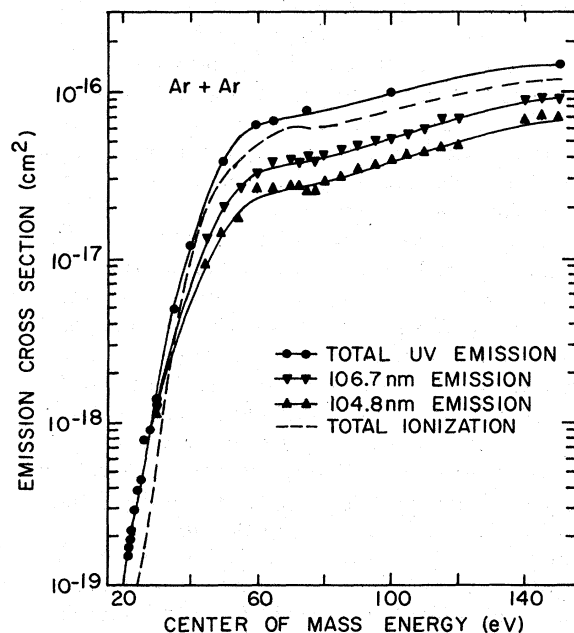


FIG. 5. Total and spectrally resolved uv emission cross sections for Ar + Ar collisions. The total ionization cross section (from Ref. 14) is shown for comparison.

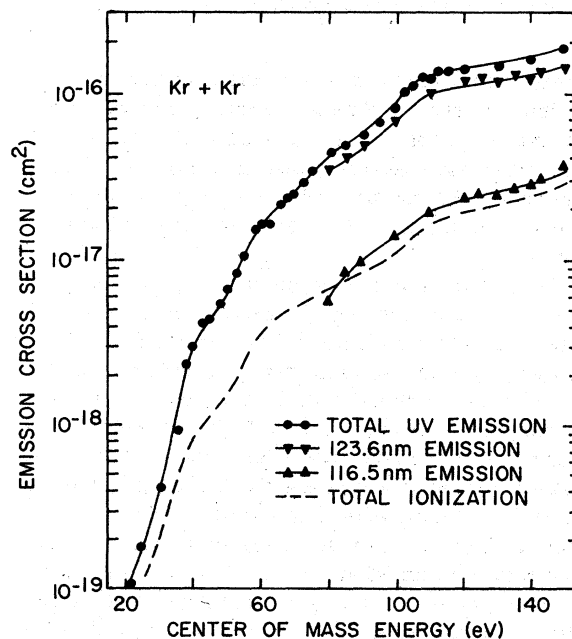


FIG. 6. Total and spectrally resolved uv emission cross sections for Kr + Kr collisions. The total ionization cross section (from Ref. 14) is shown for comparison.

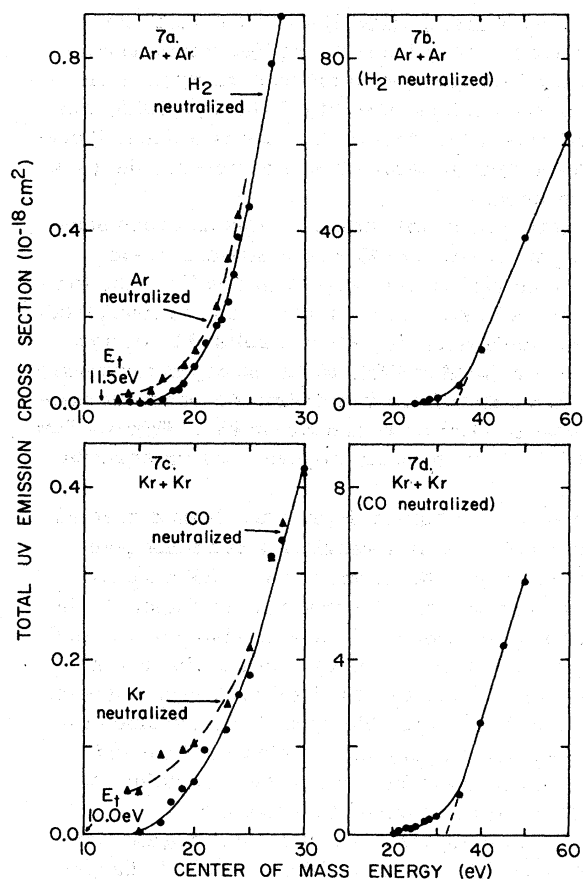


FIG. 7. Total uv emission cross sections for Ar + Ar and Kr + Kr collisions in the near-threshold regions.

transfer processes contain metastable atoms. Particularly for the Kr + Kr reaction, any reasonable extrapolation of the upper dashed curve in Fig. 7(c) would yield uv radiation below the energetic threshold for the excitation process (10.0 eV for Kr atoms and 11.5 eV for Ar) for ground-state reactants.

In fact, if the ion source electron energy is increased to above the thresholds for metastable ion formation,³ the dashed curves in Figs. 7(a) and 7(c) can be made to increase by an order of magnitude above those shown. This clearly shows the importance of the metastable ion to the metastable neutral conversion which may occur in the charge transfer reaction and the transfer of the metastable atom energy to optically decaying states in the neutral-neutral scattering collision.

The total uv emission for Ar + Ar collisions has also been studied by Haugsjaa and Amme¹² (down to 20-eV center-of-mass energy), and by Kemper, Veith, and Zehnle¹³ (down to 40-eV center-of-mass energy). Both of these measurements (which were compared with our preliminary data¹)

yielded cross sections which fell above the present results at the lower end of their respective energy ranges. We feel that trace numbers of metastable Ar atoms in the neutral beams used in these earlier studies may contribute to these observed differences.

The uncertainties in the cross sections presented here are taken to be $\pm 30\%$ down to 25-eV center-of-mass energy, below which they increase to about $\pm 50\%$ at the lowest energies investigated.

VI. DISCUSSION OF THE RESULTS

One of the striking features of the present results is that the two resonance-line emission cross sections for both Ar + Ar and Kr + Kr collisions have identical energy dependencies. In addition, it is apparent that the energy dependencies of the total ionization cross sections¹⁴ and the uv emission cross sections are very similar (see Figs. 5 and 6). This is certainly suggestive that a common interaction is operative in leading to these different final state configurations.

Brenot *et al.*¹⁵ have recently calculated molecular states of homonuclear rare gas diatomics, utilizing diabatic basis sets. (Many of the lowest excited-state potential energy curves for Ar₂ and Ar₂⁺ are shown in their Fig. 17.) They find support for their calculated potential energy curve crossings in the experimental results of several investigations. According to Brenot *et al.*, all the lowest observed inelastic processes proceed via the crossing of the diabatic incident-state curve (asymptotically the $X^1\Sigma_g$ state) with the molecular C_1 state curve (asymptotically going to two $3p^5 4s$ excited Ar atoms). This state provides a common intermediate state that then dissociates, upon subsequent crossing, into states leading to excited Ar atoms or Ar⁺ ions.

This model appears attractive in explaining the similarities we have observed between the uv emission and ionization cross sections. In fact, if one extrapolates the "straight line portion" of the observed uv emission cross section for Ar + Ar collisions [see Fig. 7(b)] to a zero intercept, the intercept occurs at about 34 ± 2 eV.¹⁶ A similar plot for the ionization cross section data yields an intercept of 32 eV. Both of these values are close to the 31-eV energy at which the $X-C_1$ crossing occurs, according to Brenot *et al.*

For the Kr + Kr system, the similarities in the uv emission and ionization cross section energy dependencies leave little doubt that a common intermediate state is again involved. Here the undulating energy dependence of both cross sections (see Fig. 6) indicates that additional channels become operative with increasing energy, as might

be expected for this more complex system. Again, however, a straight line portion of the total uv emission cross section exists (between about 35 and 50 eV) with a 32 ± 2 eV intercept [see Fig. 7(d)] even though it extends over a much smaller range of cross section magnitude than for the case of Ar+Ar collisions. Unfortunately, Brenot *et al.* have not yet developed the molecular states of Kr₂ for comparison with these data.

However, these authors feel that establishing curve crossing points by extrapolating straight line portions of such cross sections to zero intercept is rather speculative. In the first place, what evidence is available to suggest that such cross sections should exhibit linear increases at energies above the crossing energy, and if they do, over what region might this linearity be expected to persist? Secondly, it is apparent from Figs. 7(b) and 7(d) that the cross sections depart significantly from linearity in the regions below

the extrapolated intercepts.

In our preliminary disclosure of the Ar+Ar results,¹ it was shown that the total uv emission cross section exhibits a basically exponential energy dependence in the region below 40-eV center-of-mass energy, with an experimentally limited signal onset at 18 ± 2 eV. Thus, signal was observed well below the 31-eV crossing energy calculated by Brenot *et al.* It is, of course, possible to have transitions between the states involved below the crossing energy, and the basically exponential energy dependence of the transition probability in this region is not unreasonable for such quantum-mechanical phenomena.

ACKNOWLEDGMENT

The authors wish to acknowledge Herschel Neumann's support and interest in considering the theoretical aspects of the data reported.

*Present address: GTE Sylvania, HID Laboratory, Danvers, Mass. 01923.

¹H. L. Rothwell, Jr., R. C. Amme, and B. Van Zyl, *Phys. Rev. Lett.* **36**, 785 (1976).

²N. G. Utterback and G. H. Miller, *Rev. Sci. Instrum.* **32**, 1101 (1961).

³The lowest excited states of the Ar⁺ and Kr⁺ ions can be formed at ion source electron energies of about 32 and 28 eV, respectively.

⁴For these estimates, we assume the beam has cylindrical symmetry.

⁵P. O. Haugsjaa, R. C. Amme, and N. G. Utterback, *Phys. Rev. Lett.* **22**, 322 (1969).

⁶R. C. Amme and J. F. McIlwain, *J. Chem. Phys.* **45**, 1224 (1966).

⁷H. L. Rothwell, Jr., R. C. Amme, and B. Van Zyl, *J. Chem. Phys.* **68**, 4326 (1978).

⁸The LiF windows used in this experiment had a thickness of 0.2 mm.

⁹M. C. Johnson, *Rev. Sci. Instrum.* **40**, 311 (1969).

¹⁰G. H. Dunn, R. Geballe, and D. Pretzer, *Phys. Rev.* **128**, 2200 (1962).

¹¹The grating is aluminum/LiF coated to optimize the efficiency in the 100-125 nm region and is not expected to exhibit a strong efficiency dependence on wavelength in this region.

¹²P. O. Haugsjaa and R. C. Amme, *Phys. Rev. Lett.* **23**, 633 (1969).

¹³V. Kempter, F. Veith, and L. Zehnle, *Proceedings of the Ninth International Conference on the Physics of Electronic and Atomic Collisions*, edited by J. S. Risley and R. Geballe (University of Washington, Seattle, Washington, 1975), p. 617.

¹⁴The total ionization cross sections used are from P. O. Haugsjaa and R. C. Amme, *J. Chem. Phys.* **52**, 4874 (1970) for Ar+Ar collisions and R. C. Amme and P. O. Haugsjaa, *Phys. Rev.* **177**, 230 (1969) for Kr+Kr collisions.

¹⁵J. C. Brenot, D. Dhucq, J. P. Gauyacq, J. Pommier, V. Sidis, M. Barat, and E. Pollack, *Phys. Rev. A* **11**, 1245 (1975).

¹⁶A value of 32 eV was found by Kempter *et al.* (Ref. 13) even though the extrapolation spanned a considerable energy region.